

A STOCHASTIC GALERKIN METHOD FOR HAMILTON–JACOBI EQUATIONS WITH UNCERTAINTY*JINGWEI HU[†], SHI JIN[‡], AND DONGBIN XIU[§]

Abstract. We develop a class of stochastic numerical schemes for Hamilton–Jacobi equations with random inputs in initial data and/or the Hamiltonians. Since the gradient of the Hamilton–Jacobi equations gives a symmetric hyperbolic system, we utilize the generalized polynomial chaos (gPC) expansion with stochastic Galerkin procedure in random space and the Jin–Xin relaxation approximation in physical space for shock capturing. We provide an error estimate for the gPC stochastic Galerkin approximation to smooth solutions, and show that our numerical formulation preserves the symmetry and hyperbolicity of the underlying system, which allows one to efficiently quantify the uncertainty of the Hamilton–Jacobi equations due to random inputs, as demonstrated by the numerical examples.

Key words. uncertainty quantification, Hamilton–Jacobi equations, random input, relaxation schemes, generalized polynomial chaos

AMS subject classifications. 35F21, 35R60

DOI. 10.1137/140990930

1. Introduction. In recent years there has been growing interest in developing efficient and robust numerical methods for uncertainty quantification (UQ) for partial differential equations (PDE) with random inputs, where randomness can enter through initial conditions, boundary conditions, coefficients of the equations, etc. Among the most popular methods for UQ, the generalized polynomial chaos (gPC) approach [41] has received intensive attention. Combined with the stochastic Galerkin (SG) method, it has been successfully applied to many physical and engineering problems, where fast convergence can be observed if the underlying solution is sufficiently smooth. See, for example, the overviews in [15, 40].

The application of the gPC-Galerkin approach to quasilinear transport equations, in which the solutions could develop singularities is, however, quite limited. The existing works mostly focus on linear systems and scalar nonlinear problems with uncertain inputs, where the gPC-SG approach yields larger deterministic hyperbolic systems of equations [16, 33, 35]. For nonlinear systems of hyperbolic conservation laws, the lack of solution regularity not only prevents one from achieving high-order accuracy, but also poses a more serious difficulty in the loss of hyperbolicity of the resulting gPC-SG system [13]. Consequently, extra efforts are needed in order to obtain well-behaved discrete systems. One approach is to use gPC on entropy variables [32]. However, the entropy variables need be obtained by a functional minimization

*Submitted to the journal's Methods and Algorithms for Scientific Computing section October 10, 2014; accepted for publication (in revised form) July 20, 2015; published electronically September 8, 2015.

[†]<http://www.siam.org/journals/sisc/37-5/99093.html>

[‡]Department of Mathematics, Purdue University, West Lafayette, IN 47907 (hu342@purdue.edu). This author's work was partially supported by a startup grant from Purdue University.

[§]Department of Mathematics, University of Wisconsin-Madison, Madison, WI 53706, and Department of Mathematics, Institute of Natural Sciences, and MOE-LSC and SHL-MAC, Shanghai Jiao Tong University, Shanghai 200240, China (jin@math.wisc.edu). This author's work was partially supported by the NSF DMS grants 1522184 and 1107291: RNMS “KI-Net”.

[§]Department of Mathematics and Scientific Computing and Imaging Institute, The University of Utah, Salt Lake City, UT 84112 (dongbin.xiu@utah.edu). This author's work was partially supported by AFOSR FA95501410022 and NSF DMS-1418771.

procedure at every mesh point and time step. This can be computationally expensive for large scale problems. It was also shown in [32] that different entropy variables could lead to different levels of numerical oscillations due to Gibb's phenomenon in the random space.

In this paper, we identify a special class of nonlinear systems of hyperbolic conservation laws that are suitable for the gPC-SG framework—the systems from the gradient of the Hamilton–Jacobi (H–J) equations. These equations arise in a variety of applications, such as optimal control, game theory, geometric optics, front propagation, and the semiclassical limit of quantum dynamics, etc. Here we consider a general H–J equation in n space dimensions with d -dimensional random inputs

$$(1.1) \quad \partial_t u + H(\nabla_{\mathbf{x}} u, \mathbf{x}, \mathbf{z}) = 0, \quad (\mathbf{x}, \mathbf{z}, t) \in \mathbb{R}^n \times \mathbb{R}^d \times \mathbb{R}_+$$

with initial data

$$u(\mathbf{x}, \mathbf{z}, 0) = u_0(\mathbf{x}, \mathbf{z}).$$

Here $t \geq 0$ is time, H is a convex (in the first variable) Hamiltonian, $\nabla_{\mathbf{x}} = (\partial_{x_1}, \dots, \partial_{x_n})$ is the gradient with respect to $\mathbf{x} = (x_1, \dots, x_n)$, and $\mathbf{z} \in \mathbb{R}^d$ are random variables. The random variables \mathbf{z} are used to characterize the random inputs. They can be random system parameters in the equations and/or hyperparameters parameterizing certain random input processes. For deterministic problems without the random variables, this equation has been well studied both mathematically, in the framework of viscosity solutions (cf. [10, 8, 9]), and numerically using the shock capturing techniques (cf. [11, 28, 29]). The goal of this paper is to develop a robust and efficient numerical method for the random H–J equations subject to uncertain inputs, which, to the authors' best knowledge, has not been studied before.

Other than random initial data and boundary conditions, there are many applications of H–J equations where the Hamiltonian can depend on random inputs. For example, in the semiclassical limit of the Schrödinger equations, the Hamiltonian is defined by

$$(1.2) \quad H(\mathbf{p}, \mathbf{x}, \mathbf{z}) = \frac{1}{2}|\mathbf{p}|^2 + V(\mathbf{x}, \mathbf{z}),$$

where V is the potential, often obtained empirically by mean field calculations that naturally introduce uncertainty. Another application is the molecular dynamics simulation of water, where the Lennard-Jones potential contains three uncertain force-field parameters [34]. In the case of geometric optics or level set equations, the Hamiltonian takes the form

$$H(\mathbf{p}, \mathbf{x}, \mathbf{z}) = c(\mathbf{x}, \mathbf{z})|\mathbf{p}|,$$

where c is the local wave speed. It is the reciprocal of the index of refraction for the propagating medium, which is often uncertain or random. For examples, in elastic waves, c depends on Lamé parameters which could be uncertain due to measurement errors [4]. In modeling light through atmosphere, c is related to index of refraction in the air, which contains uncertainty because of errors in measurement, and the uncertain parameter could be the index of refraction itself, or pressure, temperature, and humidity of the air [1]. Consequently, it is of significant interest to study such problems and develop robust numerical methods to quantify these uncertainties.

Unlike a general nonlinear system of hyperbolic conservation laws, the equations for the gradient of the H–J equations form a *symmetric hyperbolic* system, which

is suitable for the gPC-SG approach. Our approach is a combination of a relaxation approach, originally proposed by Jin and Xin [19], for the deterministic H–J equations, and the gPC-SG approach. First, we convert the original H–J equations (1.1) into a system of conservation laws by taking their gradient, and then use the Jin–Xin relaxation approximation to construct a nonoscillatory shock capturing scheme. The advantage of the Jin–Xin relaxation is that the underlying convection terms are linear, which provides a very natural building block for the gPC approximation since the gPC system as well as its relaxation approximation *remains globally hyperbolic*. The temporal and spatial discretizations can then be done in a natural way, similar to that of deterministic systems in [21]. Our approach inherits most of the advantages of the relaxation schemes for deterministic hyperbolic conservation laws and H–J equations: simplicity and generality. Theoretically, the hyperbolicity of the new SG system is guaranteed for the general cases. Practically, the linear characteristics allow one to easily apply the standard upwind schemes without requiring a new Riemann or approximate Riemann solver (as was done in [37, 36, 31], and thus can be applied to general H–J equations as a black box.

The main goal of this paper is to demonstrate that the H–J equations are adequate for uncertainty quantification using the intrusive gPC formulation since they result in a globally hyperbolic and symmetric gPC system. This is a remarkable property not shared by general nonlinear hyperbolic systems of conservation laws. We shall not try to address the numerical difficulties of dealing with discontinuities in the random space using the global polynomial approximation. It is well known that piecewise approximations should be used in this case. These include multi-element gPC [39, 38, 17], wavelet basis [23, 24], essentially-nonoscillatory or weighted essentially-nonoscillatory interpolations [2] which may also need to be coupled with local subspace recovery techniques [5], or multiresolution approaches [3, 37]. Interested readers are referred to these references.

The rest of the paper is organized as follows: In section 2, we shall briefly present the H–J equations, their gradient system and the relaxation approximation. In section 3, we briefly review the gPC-SG method, and then give a one-dimensional (1D) (in space) error estimate of the spectral accuracy of the gPC-SG approximation under suitable regularity assumptions. We present the details of the fully discrete SG scheme for the H–J equations with random inputs, based on the relaxation approximation in section 4. Finally, we provide several numerical examples to illustrate the effectiveness of the methods in section 5.

2. Basics of H–J equations.

2.1. Equivalent form and its hyperbolicity. It is well known that, in the deterministic case, the H–J equation (1.1) has an equivalent form, in any space dimension, to a gradient system of hyperbolic conservation laws [6, 19] in the sense of zero-viscosity limit. Define

$$(2.1) \quad \mathbf{p} = (p^{(1)}, \dots, p^{(n)}) := \nabla_{\mathbf{x}} u;$$

then \mathbf{p} solves the n -dimensional system of conservation laws

$$(2.2) \quad \partial_t \mathbf{p} + \nabla_{\mathbf{x}} H(\mathbf{p}, \mathbf{x}, \mathbf{z}) = \mathbf{0}$$

or

$$(2.3) \quad \partial_t p^{(i)} + \sum_{j=1}^n \partial_{p^{(j)}} H \partial_{x_i} p^{(j)} + \partial_{x_i} H = 0, \quad i = 1, \dots, n,$$

with initial condition

$$\mathbf{p}(\mathbf{x}, \mathbf{z}, 0) = \nabla_{\mathbf{x}} u_0(\mathbf{x}, \mathbf{z}).$$

Clearly, if \mathbf{p} is known, one can recover u from \mathbf{p} by integrating the ordinary differential equation

$$(2.4) \quad \partial_t u + H(\mathbf{p}, \mathbf{x}, \mathbf{z}) = 0.$$

The equivalence of the viscosity solution between (2.4) and (1.1) was established in [19].

The system (2.3) appears to be weakly hyperbolic [27], as the Jacobian matrix could be a Jordan block at points where some of the $\partial_{p^{(k)}} H = 0$ while others do not. However, from (2.1),

$$\partial_{x_i} p^{(j)} = \partial_{x_j} p^{(i)} \quad \text{for any } i, j,$$

and by using this property in (2.3), we then obtain an equivalent system

$$(2.5) \quad \partial_t p^{(i)} + \sum_{j=1}^n \partial_{p^{(j)}} H \partial_{x_j} p^{(i)} + \partial_{x_i} H = 0, \quad i = 1, \dots, n.$$

This is clearly a symmetric hence hyperbolic system [14], as the Jacobian matrix can be diagonalized with real eigenvalues. (In fact, all the Jacobians are diagonal.) Although in each space dimension the eigenvalues of the Jacobian matrix are identical, the corresponding eigenspace has a full set of linearly independent eigenvectors.

2.2. A relaxation approximation. We adopt the Jin–Xin relaxation system [19]

$$(2.6) \quad \begin{aligned} \partial_t \mathbf{p} + \nabla_{\mathbf{x}} w &= \mathbf{0}, \\ \partial_t w + \alpha \nabla_{\mathbf{x}} \cdot \mathbf{p} &= -\frac{1}{\epsilon} (w - H(\mathbf{p}, \mathbf{x}, \mathbf{z})), \\ \partial_t u + w &= 0, \end{aligned}$$

where α is a positive constant. A Chapman–Enskog expansion on this system yields

$$\partial_t u + H(\nabla_{\mathbf{x}} u, \mathbf{x}, \mathbf{z}) = \epsilon (\alpha \Delta u - (\nabla_{\mathbf{p}} H)^T \nabla_{\mathbf{p}} \nabla_{\mathbf{p}} H - (\nabla_{\mathbf{p}} H)^T \nabla_{\mathbf{x}} H) + O(\epsilon^2)$$

which is dissipative under the so-called subcharacteristic condition [19]

$$(2.7) \quad \sqrt{\alpha} > |\nabla_{\mathbf{p}} H|.$$

This shows that, as $\epsilon \rightarrow 0^+$, the relaxation system differs from the original equation by $O(\epsilon)$. (See a rigorous justification and error estimate in [18], and the study of zero relaxation limit for space-dependent fluxes in [22, 30].) The main advantage of this relaxation system over the original system lies in the linear characteristics of the relaxation system, which will retain the hyperbolicity of the resulting SG system (see below) and therefore avoids the use of sophisticated and time-consuming Riemann solvers.

3. gPC Galerkin method.

3.1. General procedure. In the gPC expansion, one approximates the solution of a stochastic problem via an orthogonal polynomial series [41]. That is, for random variable $\mathbf{z} \in \mathbb{R}^d$, one seeks

$$p(\mathbf{x}, \mathbf{z}, t) \approx p_N(\mathbf{x}, \mathbf{z}, t) = \sum_{m=1}^M \hat{p}_m(t, \mathbf{x}) \Phi_m(\mathbf{z}), \quad M = \binom{d+N}{d},$$

where the $\{\Phi_m(\mathbf{z})\}$ are from \mathbb{P}_N^d , the d -variate orthogonal polynomials of degree up to $N \geq 1$, and orthonormal:

$$(3.1) \quad \int \Phi_i(\mathbf{z}) \Phi_j(\mathbf{z}) d\mu(\mathbf{z}) = \delta_{ij}, \quad 1 \leq i, j \leq M = \dim(\mathbb{P}_N^d).$$

Here $\mu(\mathbf{z})$ is the probability distribution function of \mathbf{z} and δ_{ij} the Kronecker delta function. The orthogonality with respect to $\mu(\mathbf{z})$ then defines the orthogonal polynomials. For example, Gaussian distribution defines Hermite polynomials, uniform distribution defines Legendre polynomials, etc. Note that when the random dimension $d > 1$, the $\{\Phi_m(\mathbf{z})\}$ are multidimensional polynomials of $\mathbf{z} = (z_1, \dots, z_d)$. An ordering scheme for a multiple index is required to reorder the polynomials into a single index m here. Typically, the graded lexicographic order is used; see, for example, section 5.2 of [40].

For PDEs with random inputs, the gPC Galerkin method seeks to satisfy the governing equation in a weak form by ensuring the residue is orthogonal to the gPC polynomial space. For a general PDE,

$$\partial_t u + \mathcal{L}(u) = 0,$$

and we then seek a gPC approximate solution $u_N = \sum_{m=1}^M \hat{u}_m \Phi_m(\mathbf{z})$ such that

$$\partial_t \hat{u}_m + \int \mathcal{L}(u_N) \Phi_m(\mathbf{z}) d\mu(\mathbf{z}) = 0, \quad m = 1, \dots, M.$$

This is a system of deterministic equations for the expansion coefficients $\{\hat{u}_m\}_{m=1}^M$. In most cases, the equations are coupled.

3.2. Accuracy of gPC-SG in one space dimension. In this subsection we state a spectral accuracy result of the gPC-SG for *smooth* solutions of the 1D H–J equation with initial random input. Such a result was proved in [13] for Burgers' equation with random initial input using a weak-strong comparison method between a general approximated solution and a smooth exact solution [12]. We adopt the proof of [13] to general scalar hyperbolic conservation laws and H–J equations with small modifications (we give relatively complete details here for convenience of the readers, although most of the presentation, except some details in the proof of Proposition 6.1, are the same as those in [13]).

Consider the 1D scalar conservation law (2.2) with random initial input

$$(3.2) \quad \partial_t p + \partial_x H(p) = 0, \quad p(x, \mathbf{z}, 0) = p_0(x, \mathbf{z}),$$

where $p = \partial_x u$ with

$$\partial_t u + H(\partial_x u) = 0, \quad u(x, \mathbf{z}, 0) = u_0(x, \mathbf{z}).$$

For convenience we only consider the periodic domain $x \in \mathcal{J} = [0, 1]_{\text{per}}$. For random space, we let $\mathbf{z} \in \mathcal{Z} \subseteq \mathbb{R}^d$, $d \geq 1$, which is equipped with a probability measure $\mu(\mathbf{z})$ and admits the gPC orthonormal basis as in (3.1). Given a smooth initial datum $p_0(x, \mathbf{z})$, there exists a T , the first time when shock develops. (Indeed, $T = -\frac{1}{\inf_x \partial_x u_0(x, \mathbf{z})}$.) We will assume $t \leq T^\delta = T - \delta < T$. We also assume the convex Hamiltonian $H \in C^2(\mathbb{R})$.

For the square entropy $p^2/2$, (3.2) admits an entropy flux $\Psi(p)$ defined by

$$\Psi'(p) = pH'(p)$$

such that the weak entropy solution to (3.2) satisfies the entropy inequality

$$\partial_t \left(\frac{1}{2} p^2 \right) + \partial_x \Psi(p) \leq 0$$

in the sense of distribution.

By applying the gPC Galerkin approximation

$$p_N(x, \mathbf{z}, t) = \sum_{m=1}^M \hat{p}_m(x, t) \Phi_m(\mathbf{z})$$

to (3.2) and conducting the Galerkin projection, we obtain

$$(3.3) \quad \partial_t \hat{p}_m + \int_{\mathcal{Z}} \partial_x H \left(\sum_{\ell=1}^M \hat{p}_\ell(t, x) \Phi_\ell(\mathbf{z}) \right) \Phi_m(\mathbf{z}) d\mu(\mathbf{z}) = 0, \quad 1 \leq m \leq M.$$

For the smooth solution of (3.3), this gives

$$\partial_t \left(\frac{1}{2} \sum_{m=1}^M \hat{p}_m^2 \right) + \partial_x \int_{\mathcal{Z}} \Psi \left(\sum_{m=1}^M \hat{p}_m(t, x) \Phi_m(\mathbf{z}) \right) d\mu(\mathbf{z}) = 0.$$

Thus the system (3.3) has the entropy

$$S(\hat{p}_1, \dots, \hat{p}_M) = \frac{1}{2} \sum_{m=1}^M \hat{p}_m^2 = \int_{\mathcal{Z}} \frac{1}{2} \left(\sum_{m=1}^M \hat{p}_m \Phi_m(\mathbf{z}) \right)^2 d\mu(\mathbf{z}) = \int_{\mathcal{Z}} \frac{1}{2} (p_N(\mathbf{z}))^2 d\mu(\mathbf{z})$$

and the entropy flux

$$G(\hat{p}_1, \dots, \hat{p}_M) = \int_{\mathcal{Z}} \Psi \left(\sum_{m=1}^M \hat{p}_m \Phi_m(\mathbf{z}) \right) d\mu(\mathbf{z}) = \int_{\mathcal{Z}} \Psi(p_N(\mathbf{z})) d\mu(\mathbf{z}).$$

For the most general case, we consider the weak entropy solution to (3.3), which satisfies the inequality

$$(3.4) \quad \partial_t \int_{\mathcal{Z}} \frac{1}{2} (p_N(\mathbf{z}))^2 d\mu(\mathbf{z}) + \partial_x \int_{\mathcal{Z}} \Psi(p_N(\mathbf{z})) d\mu(\mathbf{z}) \leq 0$$

in the sense of distribution. This implies that

$$\partial_t \int_{\mathcal{J} \times \mathcal{Z}} (p_N(\mathbf{z}))^2 dx d\mu(\mathbf{z}) \leq 0,$$

and results in the following a priori bound

$$\|p_N(\cdot, \cdot, t)\|_{L^2(\mathcal{J} \times \mathcal{Z})} \leq \|p_N(\cdot, \cdot, 0)\|_{L^2(\mathcal{J} \times \mathcal{Z})}.$$

Therefore it is natural to seek weak solutions of (3.2) in the space

$$L^\infty((0, T^\delta) : L^2(\mathcal{J} \times \mathcal{Z}))$$

as defined by the following.

DEFINITION 3.1. *A weak solution of the uncertain scalar conservation law (3.2) is a function $p_N \in L^\infty((0, T^\delta) : L^2(\mathcal{J} \times \mathcal{Z}))$ such that p_N is a polynomial of degree at most N in term of the \mathbf{z} variable (a.e. in (x, t)), such that*

$$\begin{aligned} & \int_{\mathcal{J} \times \mathcal{Z} \times (0, T^\delta)} p_N \partial_t \phi \, dx \, d\mu(\mathbf{z}) \, dt + \int_{\mathcal{J} \times \mathcal{Z} \times (0, T^\delta)} H(p_N) \partial_x \phi \, dx \, d\mu(\mathbf{z}) \, dt \\ & \quad + \int_{\mathcal{J} \times \mathcal{Z}} p_N(x, \mathbf{z}, 0) \phi(x, \mathbf{z}, 0) \, dx \, d\mu(\mathbf{z}) = 0 \end{aligned}$$

for all smooth test functions $\phi(x, \mathbf{z}, t)$ such that $\phi(x, \mathbf{z}, T^\delta) \equiv 0$.

A weak solution is an entropy weak solution if (3.4) holds true in the sense of distribution, that is,

$$\begin{aligned} & \int_{\mathcal{J} \times \mathcal{Z} \times (0, T^\delta)} \frac{1}{2} (p_N)^2 \partial_t \phi \, dx \, d\mu(\mathbf{z}) \, dt + \int_{\mathcal{J} \times \mathcal{Z} \times (0, T^\delta)} \Psi(p_N) \partial_x \phi \, dx \, d\mu(\mathbf{z}) \, dt \\ & \quad + \int_{\mathcal{J} \times \mathcal{Z}} \frac{1}{2} (p_N)^2(x, \mathbf{z}, 0) \phi(x, \mathbf{z}, 0) \, dx \, d\mu(\mathbf{z}) = 0 \end{aligned}$$

for all smooth test functions $\phi(x, \mathbf{z}, t)$ such that $\phi(x, \mathbf{z}, T^\delta) \equiv 0$.

We now define

$$u_N(x, \mathbf{z}, t) = \int_0^x p_N(x', \mathbf{z}, t) \, dx',$$

and state the main theorem about the accuracy of the gPC Galerkin solution p_N and u_N .

THEOREM 3.2. *Let $\Pi_N p$ be the N th degree orthogonal polynomial projection of p and assume*

$$(3.5) \quad \begin{aligned} \|p - \Pi_N p\|_{L^2(\mathcal{J} \times \mathcal{Z})} &\lesssim N^{-k}, \\ \|\partial_x(p - \Pi_N p)\|_{L^2(\mathcal{J} \times \mathcal{Z})} &\lesssim N^{-k} \end{aligned}$$

for some $k > 0$. Let us also assume that p_N is bounded uniformly in N ; then there exists a constant $D_k^\delta \geq 0$ such that for $t \leq T^\delta$,

$$(3.6) \quad \|p_N(t) - p(t)\|_{L^2(\mathcal{J} \times \mathcal{Z})}^2 \leq D_k^\delta \left(\|p_N(0) - p(0)\|_{L^2(\mathcal{J} \times \mathcal{Z})}^2 + \frac{1}{N^k} \right),$$

$$(3.7) \quad \|u_N(t) - u(t)\|_{H^1(\mathcal{J} \times \mathcal{Z})}^2 \leq D_k^\delta \left(\|u_N(0) - u(0)\|_{H^1(\mathcal{J} \times \mathcal{Z})}^2 + \frac{1}{N^k} \right).$$

We leave the details of the proof to the appendix.

Remark 3.3. The N^{-k} convergence of the orthogonal projection error is a common assumption used in spectral error analysis. It is rather mild and often can be satisfied when p lies in a Sobolev space H^k .

Remark 3.4. The assumption on the uniform boundedness of p_N is not proven. We need this assumption so that H'' is bounded, which is needed in Proposition 6.1. In the case of the Burgers equation $H(u) = u^2/2$, which is the case studied in [13], the boundedness of H'' is automatically satisfied.

4. The gPC-Galerkin relaxation scheme. In the gPC Galerkin scheme for system (2.6), one seeks polynomial approximations of the following form:

$$(4.1) \quad \begin{aligned} \mathbf{p}_N(\mathbf{x}, \mathbf{z}, t) &= \sum_{m=1}^M \hat{\mathbf{p}}_m(t, \mathbf{x}) \Phi_m(\mathbf{z}), \\ w_N(\mathbf{x}, \mathbf{z}, t) &= \sum_{m=1}^M \hat{w}_m(t, \mathbf{x}) \Phi_m(\mathbf{z}), \\ H_N(\mathbf{x}, \mathbf{z}, t) &= \sum_{m=1}^M \hat{H}_m(t, \mathbf{x}) \Phi_m(\mathbf{z}), \\ u_N(\mathbf{x}, \mathbf{z}, t) &= \sum_{m=1}^M \hat{u}_m(t, \mathbf{x}) \Phi_m(\mathbf{z}). \end{aligned}$$

Let

$$\hat{\mathbf{p}} = (\hat{\mathbf{p}}_1, \dots, \hat{\mathbf{p}}_M)^T, \quad \hat{\mathbf{w}} = (\hat{w}_1, \dots, \hat{w}_M)^T, \quad \hat{\mathbf{H}} = (\hat{H}_1, \dots, \hat{H}_M)^T, \quad \hat{\mathbf{u}} = (\hat{u}_1, \dots, \hat{u}_M)^T$$

be the coefficient vectors. Define

$$\mathbf{r} = (\Phi_1, \dots, \Phi_M)^T.$$

One can insert (4.1) into the system (2.5) and then conduct the Galerkin projection on the governing equation to get

$$(4.2) \quad \partial_t \hat{\mathbf{p}}^{(i)} + \sum_{j=1}^n \int \partial_{p^{(j)}} H(\mathbf{p}_N, \mathbf{x}, \mathbf{z}) \mathbf{r} \mathbf{r}^T d\mu(\mathbf{z}) \partial_{x_j} \hat{\mathbf{p}}^{(i)} + \int \partial_{x_i} H(\mathbf{p}_N, \mathbf{x}, \mathbf{z}) \mathbf{r} d\mu(\mathbf{z}) = \mathbf{0},$$

where $\mathbf{0}$ is the M -dimensional zero vector. Clearly, in the above equation, the Jacobian matrices

$$(4.3) \quad \int \partial_{p^{(j)}} H(\mathbf{p}_N, \mathbf{x}, \mathbf{z}) \mathbf{r} \mathbf{r}^T d\mu(\mathbf{z})$$

for all $1 \leq j \leq n$ are symmetric (here the integration over \mathbf{z} is taken entrywise for the matrices). Therefore, the gPC-SG system (4.2) is *symmetric hyperbolic*, which gives a well-posed system amicable to the use of the standard shock capturing methods.

One could also apply the gPC expansion directly to the original H–J equation (1.1) and conduct the Galerkin projection to obtain a system that can be solved by some shock capturing methods (such methods are usually constructed via the connection with the gradient system (2.2) as well).

4.1. The relaxation scheme. While there are many possible shock capturing methods that can be used to solve (4.2), here we employ the relaxation approach (2.6), not only for its simplicity (no Riemann or approximate solver is needed) but also for its desirable theoretical property—under the semilinear relaxation approximation the gPC system takes the same (but vectorized) form as the original relaxation system (2.6), thus retaining the global hyperbolicity under the relaxation approximation. This offers an intriguing regularization which could be useful in other applications such as a system of conservation laws [20]. Furthermore, in many applications, e.g., in the semiclassical approximation of the Schrödinger equation, u represents the phase

while \mathbf{p} represents the velocity, both of which are of physical importance; thus it is advantageous to have a method that solves for both quantities. The relaxation scheme offers such a possibility.

By inserting (4.1) into the relaxation system (2.6) and then conducting the Galerkin projection on the governing equation, we obtain

$$(4.4) \quad \begin{aligned} \partial_t \hat{\mathbf{p}} + \nabla_{\mathbf{x}} \hat{\mathbf{w}} &= \mathbf{0}, \\ \partial_t \hat{\mathbf{w}} + \alpha \nabla_{\mathbf{x}} \cdot \hat{\mathbf{p}} &= -\frac{1}{\epsilon} (\hat{\mathbf{w}} - \hat{\mathbf{H}}), \\ \partial_t \hat{\mathbf{u}} + \hat{\mathbf{w}} &= \mathbf{0}. \end{aligned}$$

The relaxation system always has a complete set of linearly independent eigenvectors. The hyperbolicity of the SG (4.4) is straightforward.

The relaxation scheme consists of the following two steps:

- *Convection step:*

$$(4.5) \quad \begin{aligned} \partial_t \hat{\mathbf{p}} + \nabla_{\mathbf{x}} \hat{\mathbf{w}} &= \mathbf{0}, \\ \partial_t \hat{\mathbf{w}} + \alpha \nabla_{\mathbf{x}} \cdot \hat{\mathbf{p}} &= \mathbf{0}, \\ \partial_t \hat{\mathbf{u}} + \hat{\mathbf{w}} &= \mathbf{0}. \end{aligned}$$

- *Relaxation step:*

$$\hat{\mathbf{w}} = \hat{\mathbf{H}}.$$

Remark 4.1. The definition of $\hat{\mathbf{H}}$ will depend on the specific form of H , as will be discussed later.

Remark 4.2. Since $\hat{\mathbf{H}}$ in (4.4) is not the same matrix as $\nabla_{\mathbf{p}} H$, one might need a different constant α in (4.4) from that in (2.6). However, since the Jacobian matrix (4.3) has eigenvalues that can be bounded by the maximum of $|\partial_{p^{(j)}} H(\mathbf{p}_N, \mathbf{x}, \mathbf{z})|$ [42], one can use the same α . Since α contributes to the numerical viscosity, one can make α space and time dependent by satisfying the subcharacteristic condition (2.7) locally. We do not elaborate on this in the current paper.

Remark 4.3. One could apply gPC Galerkin directly on system (2.2) and then take a relaxation approximation. This will end up with the same system (4.4).

4.2. Spatial discretization. For clear exposition purposes we employ the second-order MUSCL [25] (monotonic upstream-centered scheme for conservation laws) discretization for the convection step (4.5). We will only present the two spatial dimensions case. For details, see [19].

The two dimensional (2D) system of (4.5) is

$$(4.6) \quad \begin{aligned} \partial_t \hat{\mathbf{p}}^{(1)} + \partial_x \hat{\mathbf{w}} &= \mathbf{0}, \\ \partial_t \hat{\mathbf{p}}^{(2)} + \partial_y \hat{\mathbf{w}} &= \mathbf{0}, \\ \partial_t \hat{\mathbf{w}} + \alpha \partial_x \hat{\mathbf{p}}^{(1)} + \alpha \partial_y \hat{\mathbf{p}}^{(2)} &= \mathbf{0}, \\ \partial_t \hat{\mathbf{u}} + \hat{\mathbf{w}} &= \mathbf{0}. \end{aligned}$$

For spatial discretization, we choose the spatial grids $(x_{i+1/2}, y_{j+1/2})$ with a uniform mesh size $\Delta x = x_{i+1/2} - x_{i-1/2}$ and $\Delta y = y_{j+1/2} - y_{j-1/2}$. We denote the cell average in $c_{ij} = [x_{i-1/2}, x_{i+1/2}] \times [y_{j-1/2}, y_{j+1/2}]$ as

$$\hat{\mathbf{u}}_{ij} = \frac{1}{\Delta x \Delta y} \int_{x_{i-1/2}}^{x_{i+1/2}} \int_{y_{j-1/2}}^{y_{j+1/2}} \hat{\mathbf{u}}(x, y) dx dy,$$

and similarly for other quantities. Integrating (4.6) over cell c_{ij} , we obtain

$$\begin{aligned}\partial_t \hat{\mathbf{p}}_{ij}^{(1)} + \frac{1}{\Delta x} (\hat{\mathbf{w}}_{i+1/2,j} - \hat{\mathbf{w}}_{i-1/2,j}) &= \mathbf{0}, \\ \partial_t \hat{\mathbf{p}}_{ij}^{(2)} + \frac{1}{\Delta y} (\hat{\mathbf{w}}_{i,j+1/2} - \hat{\mathbf{w}}_{i,j-1/2}) &= \mathbf{0}, \\ \partial_t \hat{\mathbf{w}}_{ij} + \frac{\alpha}{\Delta x} (\hat{\mathbf{p}}_{i+1/2,j}^{(1)} - \hat{\mathbf{p}}_{i-1/2,j}^{(1)}) + \frac{\alpha}{\Delta y} (\hat{\mathbf{p}}_{i,j+1/2}^{(2)} - \hat{\mathbf{p}}_{i,j-1/2}^{(2)}) &= \mathbf{0}, \\ \partial_t \hat{\mathbf{u}}_{i+1/2,j} + \hat{\mathbf{w}}_{i+1/2,j} &= \mathbf{0},\end{aligned}$$

where the numerical flux $\hat{\mathbf{w}}_{i+1/2,j}$ is the cell average in the y variable and pointwise value at $x_{i+1/2}$ (similarly for the other fluxes) and defined by the MUSCL scheme [26] as

$$\begin{aligned}\hat{\mathbf{w}}_{i+1/2,j} &= \frac{1}{2} (\hat{\mathbf{w}}_{ij} + \hat{\mathbf{w}}_{i+1,j}) - \frac{\sqrt{\alpha}}{2} (\hat{\mathbf{p}}_{i+1,j}^{(1)} - \hat{\mathbf{p}}_{ij}^{(1)}) \\ &\quad + \frac{\sqrt{\alpha}}{4} \Delta x (\sigma_{ij}^{x,+} + \sigma_{i+1,j}^{x,-}).\end{aligned}$$

Here

$$\begin{aligned}\sigma_{ij}^{x,\pm} &= \frac{1}{\Delta x} \left(\hat{\mathbf{p}}_{i+1,j}^{(1)} \pm \frac{1}{\sqrt{\alpha}} \hat{\mathbf{w}}_{i+1,j} - \hat{\mathbf{p}}_{ij}^{(1)} \mp \frac{1}{\sqrt{\alpha}} \hat{\mathbf{w}}_{ij} \right) \phi(\theta_{ij}^{x,\pm}), \\ \theta_{ij}^{x,\pm} &= \frac{\hat{\mathbf{p}}_{ij}^{(1)} \pm \frac{1}{\sqrt{\alpha}} \hat{\mathbf{w}}_{ij} - \hat{\mathbf{p}}_{i-1,j}^{(1)} \mp \frac{1}{\sqrt{\alpha}} \hat{\mathbf{w}}_{i-1,j}}{\hat{\mathbf{p}}_{i+1,j}^{(1)} \pm \frac{1}{\sqrt{\alpha}} \hat{\mathbf{w}}_{i+1,j} - \hat{\mathbf{p}}_{ij}^{(1)} \mp \frac{1}{\sqrt{\alpha}} \hat{\mathbf{w}}_{ij}},\end{aligned}$$

are the limited slope obtained by applying the van Leer slope limiter

$$\phi(\theta) = \frac{|\theta| + \theta}{1 + |\theta|}.$$

5. Numerical examples. In this section, we present several numerical examples to illustrate the effectiveness of our methods. The randomness/uncertainty can enter the problem through either initial conditions or Hamiltonians. For simplicity, we will always assume a 1D random variable z obeying the uniform distribution on $[-1, 1]$; thus the Legendre polynomial chaos are used as the gPC basis. Our examples include both 1D and 2D nonlinear systems. The purpose is to clearly demonstrate the effectiveness of our method—the strong hyperbolicity of the gPC Galerkin systems. Therefore, we do not pursue more complicated examples involving multiple random variables as it can be done in a very straightforward manner.

In the following, the first-order scheme refers to upwind in space and forward Euler in time; the second-order scheme refers to the MUSCL scheme (with the van Leer limiter) in space and Heun's method in time. The initial condition is chosen consistently as $\mathbf{p}_0(\mathbf{x}, z) = \nabla_{\mathbf{x}} u_0(\mathbf{x}, z)$ and $w_0(\mathbf{x}, z) = H(\mathbf{p}_0, \mathbf{x}, z)$. The periodic boundary condition is assumed except for the first example. Two metrics are typically used to quantify the difference in the numerical solution, $u^h(\mathbf{x}, z, t)$, and the reference solution, $u(\mathbf{x}, z, t)$: the difference in mean and in standard deviation, with l^1 -norm in \mathbf{x} :

$$\begin{aligned}e_{\text{mean}}(t) &= \|\mathbb{E}[u^h] - \mathbb{E}[u]\|_{l^1}, \\ e_{\text{std}}(t) &= \|\sigma[u^h] - \sigma[u]\|_{l^1},\end{aligned}$$

where $\mathbb{E}[u^h] = \hat{u}_1^h$, $\sigma[u^h] = \sqrt{\sum_{m=2}^M (\hat{u}_m^h)^2}$, and (u_1^h, \dots, u_M^h) are the gPC coefficients

for u^h ; $\mathbb{E}[u]$ and $\sigma[u]$ for the reference solution are computed by numerical quadrature. Finally, the l^1 norm for a function $f(x)$ is defined as $\|f(x)\|_{l^1} = \sum_{x_i} |f(x_i)|\Delta x$.

5.1. 1D examples.

Example 1 (1D Burgers equation with random Riemann initial data). Consider

$$(5.1) \quad u_t + H(u_x) = 0, \quad H(p) = \frac{1}{2}p^2, \quad x \in [0, 1],$$

with randomly perturbed initial data

$$u_0(x, z) = \begin{cases} (u_l + \sigma z)x, & x \leq 0.5, \\ (u_r + \sigma z)x + 0.5(u_l - u_r), & x > 0.5, \end{cases} \quad \sigma = 0.1.$$

This Hamiltonian, in the form of (1.2), arises in the semiclassical limit of the linear Schrödinger equation. The derivative of (5.1) is clearly the Burgers equation.

Here we need to handle the nonlinear Hamiltonian H in the context of the SG approach. The corresponding gPC approximation based on p_N is given by

$$H(p) \approx H(p_N) = \frac{1}{2} \sum_{i=0}^N \sum_{j=0}^N \hat{p}_i \hat{p}_j \Phi_i(z) \Phi_j(z),$$

which is not in \mathbb{P}_N , but always in $L^2_{d\mu(z)}$, where

$$L^2_{d\mu(z)} = \left\{ f : \mathcal{Z} \rightarrow \mathbb{R} \mid \mathbb{E}[f^2] = \int_{\mathcal{Z}} f^2(z) d\mu(z) < \infty \right\}.$$

We then approximate $H(p)$ by its orthogonal projection H_N on \mathbb{P}_N , whose gPC coefficients are defined as follows:

$$(5.2) \quad \hat{H}_k = \frac{1}{2} \sum_{i=0}^N \sum_{j=0}^N \hat{p}_i \hat{p}_j S_{ijk}, \quad 0 \leq k \leq N,$$

where

$$S_{ijk} = \int \Phi_i(z) \Phi_j(z) \Phi_k(z) d\mu(z), \quad 0 \leq i, j, k \leq N.$$

We choose $\alpha = 1.5$, $N = 7$ (highest degree in the gPC expansion), $N_x = 200$, CFL = 0.8 for the first-order scheme, CFL = 0.4 for the second-order scheme. We consider two cases and compare the numerical solutions with the reference solutions at $t = 0.3$ (20 Gauss-Legendre quadrature points are used to evaluate the mean and standard deviation of the exact solution).

Case 1 (shock): $u_l = 1$, $u_r = -1$. The exact p and u are given by

$$\begin{aligned} p(x, z, t) &= \begin{cases} u_l + \sigma z, & x \leq 0.5 + \sigma z t, \\ u_r + \sigma z, & x > 0.5 + \sigma z t; \end{cases} \\ u(x, z, t) &= \begin{cases} (u_l + \sigma z)x - \frac{(u_l + \sigma z)^2}{2}t, & x \leq 0.5 + \sigma z t, \\ (u_r + \sigma z)x + 0.5(u_l - u_r) - \frac{(u_r + \sigma z)^2}{2}t, & x > 0.5 + \sigma z t. \end{cases} \end{aligned}$$

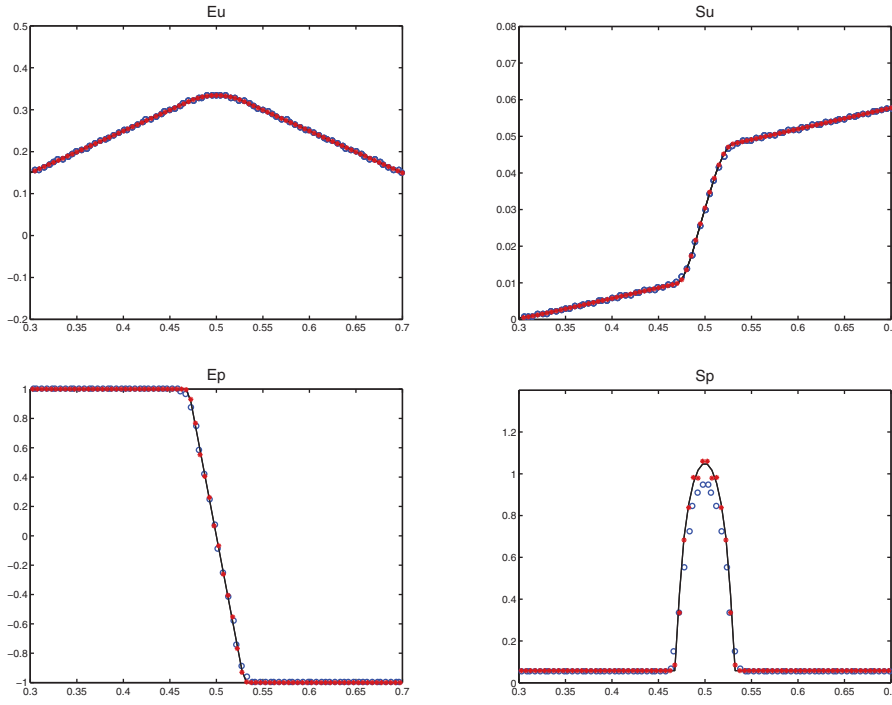


FIG. 1. Example 1, case 1 (shock). Solid line: reference solution; circle: first-order scheme; star: second-order scheme. Top: mean and standard deviation of u ; bottom: mean and standard deviation of $p = u_x$. All solutions are zoomed into $x \in [0.3, 0.7]$.

The solutions are plotted in Figure 1. In this case, there is a shock in p along the x direction. After taking the average in z , the sharp discontinuity is smoothed out.

Case 2 (rarefaction): $u_l = -1$, $u_r = 1$. The exact p and u are given by

$$p(x, z, t) = \begin{cases} u_l + \sigma z, & x \leq 0.5 + (u_l + \sigma z)t, \\ \frac{x-0.5}{t}, & 0.5 + (u_l + \sigma z)t < x \leq 0.5 + (u_r + \sigma z)t, \\ u_r + \sigma z, & x > 0.5 + (u_r + \sigma z)t; \end{cases}$$

$$u(x, z, t) = \begin{cases} (u_l + \sigma z)x - \frac{(u_l + \sigma z)^2}{2}t, & x \leq 0.5 + (u_l + \sigma z)t, \\ 0.5(u_l + \sigma z) + \frac{1}{2t}(x - 0.5)^2, & 0.5 + (u_l + \sigma z)t < x \leq 0.5 + (u_r + \sigma z)t, \\ (u_r + \sigma z)x + 0.5(u_l - u_r) - \frac{(u_r + \sigma z)^2}{2}t, & x > 0.5 + (u_r + \sigma z)t. \end{cases}$$

The solutions are plotted in Figure 2. In this case, a rarefaction wave will form in p along the x direction.

In either case, we obtain good agreement between the numerical solutions and the reference solutions. We also conduct the convergence test with respect to the gPC order: in the rarefaction case (Figure 3, right), the error decays very rapidly in N and then saturates once the spatial error dominates. Note that the error in u is smaller than in p since the former has better regularity. In the shock case (Figure 3, left), the error decreases very slowly because of the discontinuities in the solution. We then fix a relatively large N and test the convergence regarding the spatial discretization.

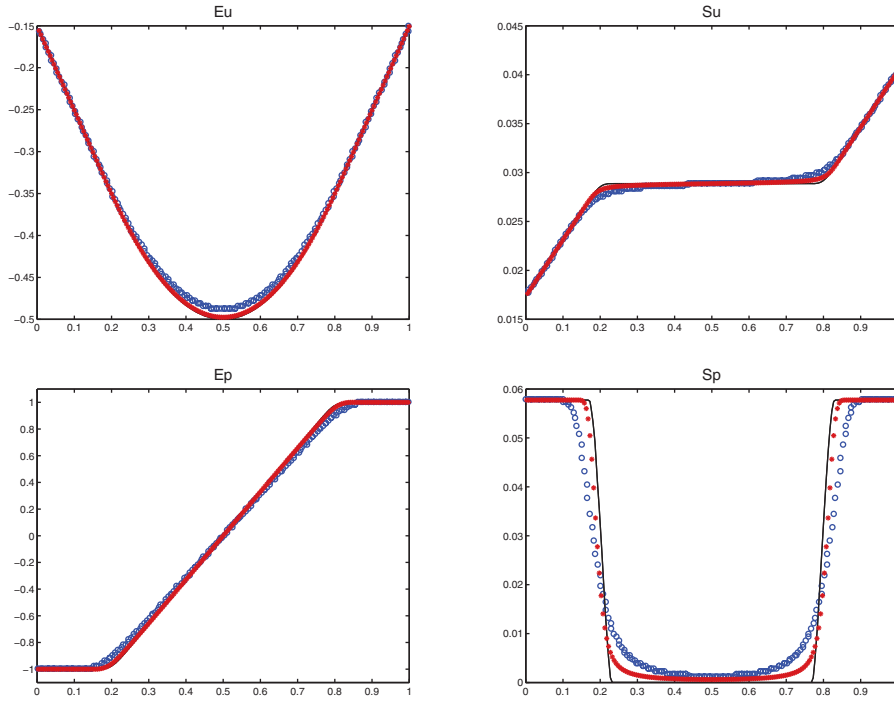


FIG. 2. *Example 1, case 2 (rarefaction).* Solid line: reference solution; circle: first-order scheme; star: second-order scheme. Top: mean and standard deviation of u ; bottom: mean and standard deviation of $p = u_x$.

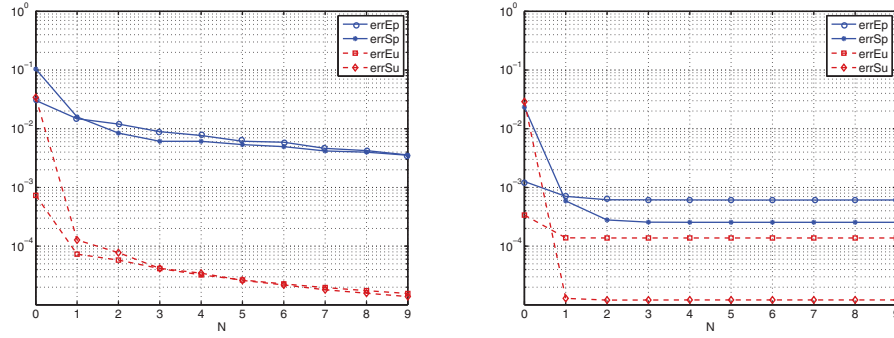


FIG. 3. *Example 1, convergence test.* Error versus gPC-order N . Second-order scheme is used with $\Delta x = 6.25e-4$, $\Delta t = 2e-4$. Left: case 1 (shock); right: case 2 (rarefaction).

The results for the rarefaction case are shown in Figure 4. Due to the finite regularity of the solution, the second-order scheme can only achieve first-order accuracy.

Remark 5.1. The convergence of the global gPC suffers severely for the shock case and is not shown. This is a well-known case where piecewise basis shall be adopted, as discussed in the introduction. Since this is not the focus of this paper, we leave it for future work.

Example 2 (1D Burgers' equation with random smooth initial data). Consider

$$u_t + H(u_x) = 0, \quad H(p) = \frac{1}{2}p^2, \quad x \in [0, 2\pi],$$

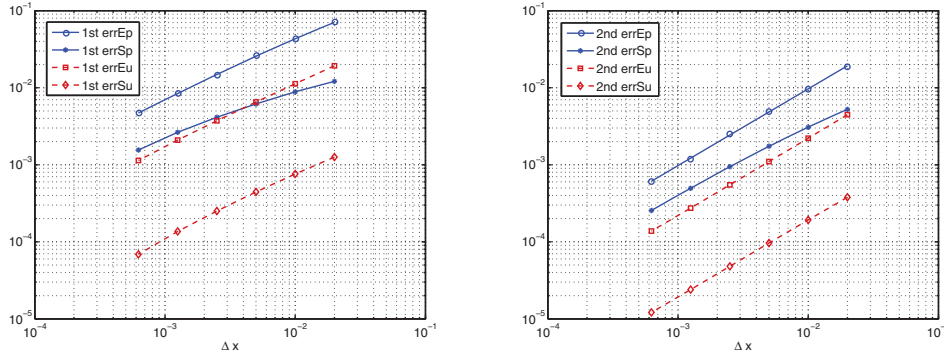


FIG. 4. Example 1, case 2 (rarefaction). Convergence test. Error versus spatial discretization Δx . $N = 9$. $\Delta t = 2e - 4$. Left: first-order scheme; right: second-order scheme.

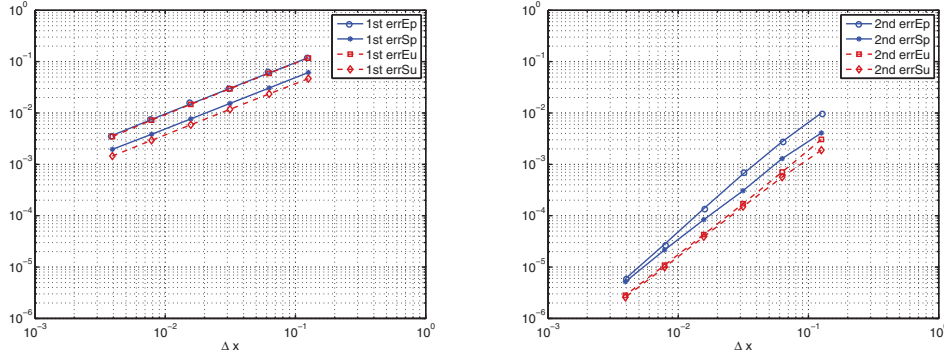


FIG. 5. Example 2, convergence test. Error versus spatial discretization Δx . $N = 9$. $\Delta t = 0.001$. Left: first-order scheme; right: second-order scheme.

with random smooth initial data

$$u_0(x, z) = \sin(x + \sigma z), \quad \sigma = 0.6.$$

The deterministic version of this problem (when $\sigma = 0$) was used as a test example in [7].

The solution of u develops a caustic at time $t = 1$. When $t = 0.5$, it is still smooth, and we can construct the exact solution by the method of characteristics: solve $x = x_0 + \cos(x_0 + \sigma z)t$ for $x_0 = x_0(x, z, t)$, then $p(x, z, t) = \cos(x_0 + \sigma z)$ and $u(x, z, t) = \sin(x_0 + \sigma z) + \frac{\cos^2(x_0 + \sigma z)}{2}t$. Similar convergence tests were conducted to verify the accuracy of the scheme. The results are gathered in Figures 5 and 6, from which we clearly observe the first- and second-order convergence in space, and spectral convergence with respect to gPC order (the error saturates after $N = 6$ due to the numerical error in spatial and temporal discretizations).

After $t = 1$, a shock forms in $p = u_x$. We choose $\alpha = 1.1$, $N = 7$, $N_x = 200$, CFL = 0.8 for the first-order scheme, CFL = 0.4 for the second-order scheme, and compare our solution with the reference solution at $t = 1.5$. The reference solution is computed based on stochastic collocation using the second-order scheme with $N_x = 800$, CFL = 0.4, and 20 Gauss–Legendre quadrature points in the random space. See Figure 7.

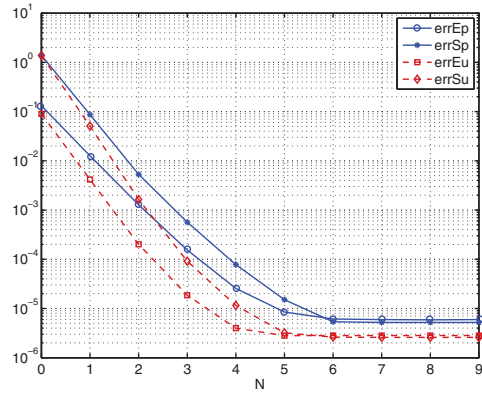


FIG. 6. Example 2, convergence test. Error versus gPC-order N . Second-order scheme is used with $\Delta x = 0.0039$, $\Delta t = 0.001$.

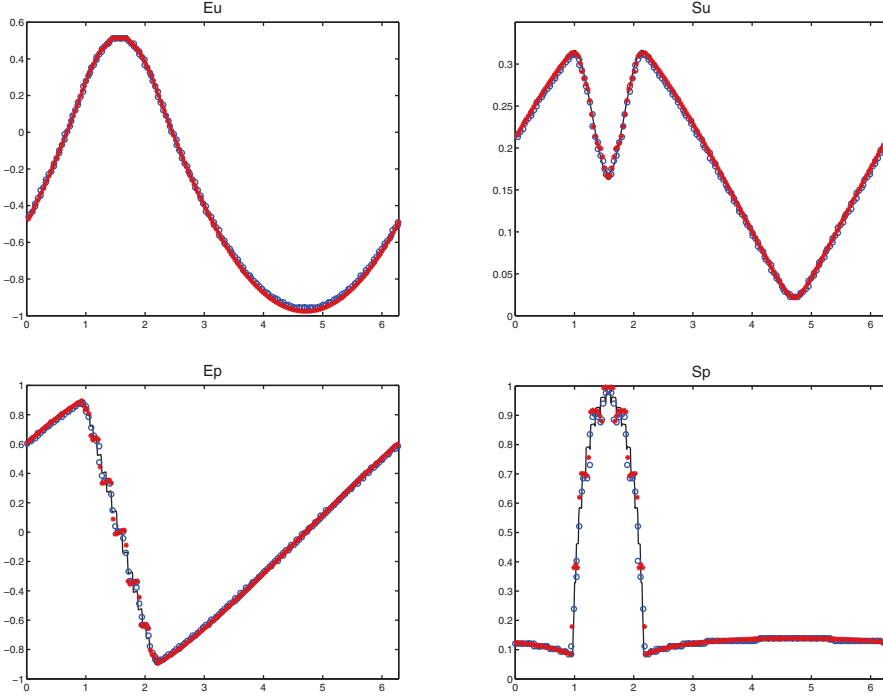


FIG. 7. Example 2. Solid line: reference solution; circle: first-order scheme; star: second-order scheme. Top: mean and standard deviation of u ; bottom: mean and standard deviation of $p = u_x$.

Note that the zigzag behavior in the mean of p is due to the pitfall of high order polynomial interpolation of a discontinuity solution in the random space, as discussed (and fixed) in [5]. For reference, we also plot the deterministic solutions (i.e., $\sigma = 0$, no uncertainty in the initial condition) in Figure 8.

Example 3 (1D Burgers' equation with random potential). Consider

$$u_t + H(u_x, x, z) = 0, \quad H(p, x, z) = \frac{1}{2}p^2 + V(x, z), \quad x \in [0, 2\pi],$$

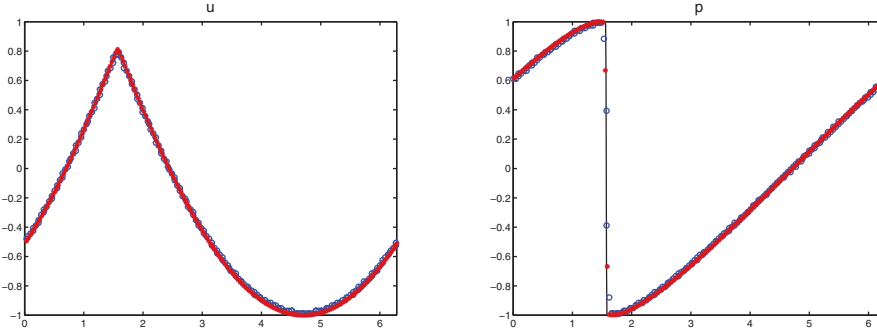


FIG. 8. Example 2. $\sigma = 0$ (no uncertainty in initial condition). Solid line: reference solution; circle: first-order scheme; star: second-order scheme. Left: u ; right: $p = u_x$.

with random potential

$$(5.3) \quad V(x, z) = \frac{(1 + \sigma z)}{\pi^2} (x - \pi)^2, \quad \sigma = 0.3,$$

and deterministic initial data

$$u_0(x) = \sin x.$$

Here the gPC expansion coefficients for H , \hat{H}_k , can be computed the same as in (5.2) but with an extra term:

$$\hat{H}_k = \frac{1}{2} \sum_{i=0}^N \sum_{j=0}^N \hat{p}_i \hat{p}_j S_{ijk} + \hat{V}_k, \quad 0 \leq k \leq N,$$

where the \hat{V}_k are the gPC expansion coefficients of the potential (5.3).

We choose $\alpha = 4$, $N = 7$, $N_x = 200$, CFL = 0.8 for the first-order scheme, CFL = 0.4 for the second-order scheme, and compare our solution with the reference solution at $t = 1.5$. The reference solution is computed based on the stochastic collocation using the second-order scheme with $N_x = 800$, CFL = 0.4, and 20 Gauss–Legendre quadrature points in the random space. See Figure 9.

Example 4 (1D Eikonal equation with random wave speed). Consider

$$u_t + H(u_x, x, z) = 0, \quad H(p, x, z) = c(x, z)|p|, \quad x \in [0, 2\pi],$$

with random wave speed

$$c(x, z) = 1 + \sigma z, \quad \sigma = 0.2,$$

and deterministic initial data

$$u_0(x, z) = \sin x.$$

In this and Examples 6 and 7, the Hamiltonian H is not a polynomial in p , so there is no simple way to evaluate its gPC coefficients. Therefore, we approximate the following integral directly using the Gauss quadrature rule:

$$\hat{H}_k = \int H \left(\sum_{i=0}^N \hat{p}_i \Phi_i(z) \right) \Phi_k(z) d\mu(z).$$

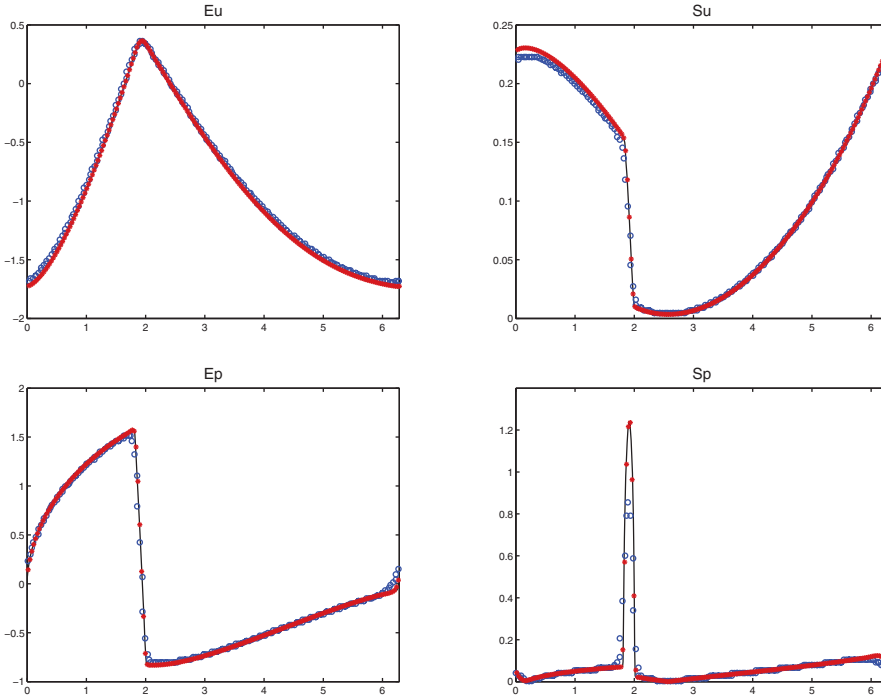


FIG. 9. Example 3. Solid line: reference solution; circle: first-order scheme; star: second-order scheme. Top: mean and standard deviation of u ; bottom: mean and standard deviation of $p = u_x$.

We choose $\alpha = 1.5$, $N = 7$, $N_x = 200$, $\text{CFL} = 0.8$ for the first-order scheme, $\text{CFL} = 0.4$ for the second-order scheme, and compare our solution with the reference solution at $t = 1$. The reference solution is computed based on the stochastic collocation using the second-order scheme with $N_x = 800$, $\text{CFL} = 0.4$, and 20 Gauss-Legendre quadrature points in the random space. See Figure 10.

5.2. 2D examples.

Example 5 (2D Burgers' equation with random potential). Consider

$$u_t + H(u_x, u_y, x, y, z) = 0, \quad H(p, q, x, y, z) = \frac{1}{2}(p+q+1)^2 + V(x, y, z), \quad (x, y) \in [-2, 2]^2,$$

with random potential

$$(5.4) \quad V(x, y, z) = \frac{(1 + \sigma z)}{8}(x^2 + y^2), \quad \sigma = 0.5,$$

and deterministic initial data

$$u_0(x, y) = -\cos\left(\frac{\pi}{2}(x + y)\right).$$

Here the Hamiltonian is a quadratic function which can be computed similarly as those in the 1D examples:

$$\hat{H}_k = \frac{1}{2} \sum_{i=0}^N \sum_{j=0}^N \hat{r}_i \hat{r}_j S_{ijk} + \tilde{V}_k, \quad 0 \leq k \leq N,$$

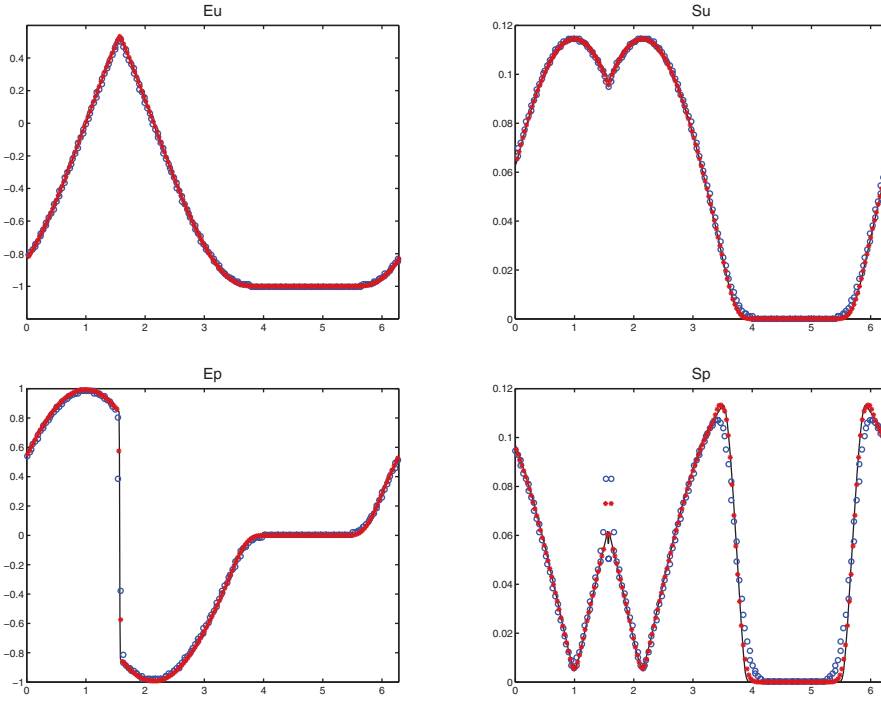


FIG. 10. Example 4. Solid line: reference solution; circle: first-order scheme; star: second-order scheme. Top: mean and standard deviation of u ; bottom: mean and standard deviation of $p = u_x$.

where $\hat{r}_0 = \hat{p}_0 + \hat{q}_0 + 1$, $\hat{r}_i = \hat{p}_i + \hat{q}_i$, $i \neq 0$, and \hat{V}_k is the gPC coefficient of the potential (5.4).

We choose $\alpha = 50$, $N = 7$, $N_x = N_y = 40$, $\text{CFL} = 0.8$ for the first-order scheme, $\text{CFL} = 0.4$ for the second-order scheme, and compare our solution with the reference solution at $t = \frac{1.5}{\pi^2}$. The reference solution is computed based on the stochastic collocation using the second-order scheme with $N_x = 160$, $\text{CFL} = 0.4$, and 20 Gauss–Legendre quadrature points in the random space. The results are shown in Figures 11 and 12.

Example 6 (2D Eikonal equation with random initial data). Consider

$$u_t + H(u_x, u_y) = 0, \quad H(p) = -\sqrt{p^2 + q^2 + 1}, \quad (x, y) \in [0, 1]^2,$$

with random initial data

$$u_0(x, y, z) = -\frac{1 + \sigma z}{4} [\cos(2\pi x) - 1][\cos(2\pi y) - 1] + 1.$$

The deterministic version of this problem was first considered in [28]. We choose $\alpha = 1.1$, $N = 7$, $N_x = N_y = 40$, $\text{CFL} = 0.8$ for the first-order scheme, $\text{CFL} = 0.4$ for the second-order scheme, and compare our solution with the reference solution at $t = 0.3$. The reference solution is computed based on the stochastic collocation using the second-order scheme with $N_x = N_y = 160$, $\text{CFL} = 0.4$, and 20 Gauss–Legendre quadrature points in the random space. The results are shown in Figures 13 and 14.

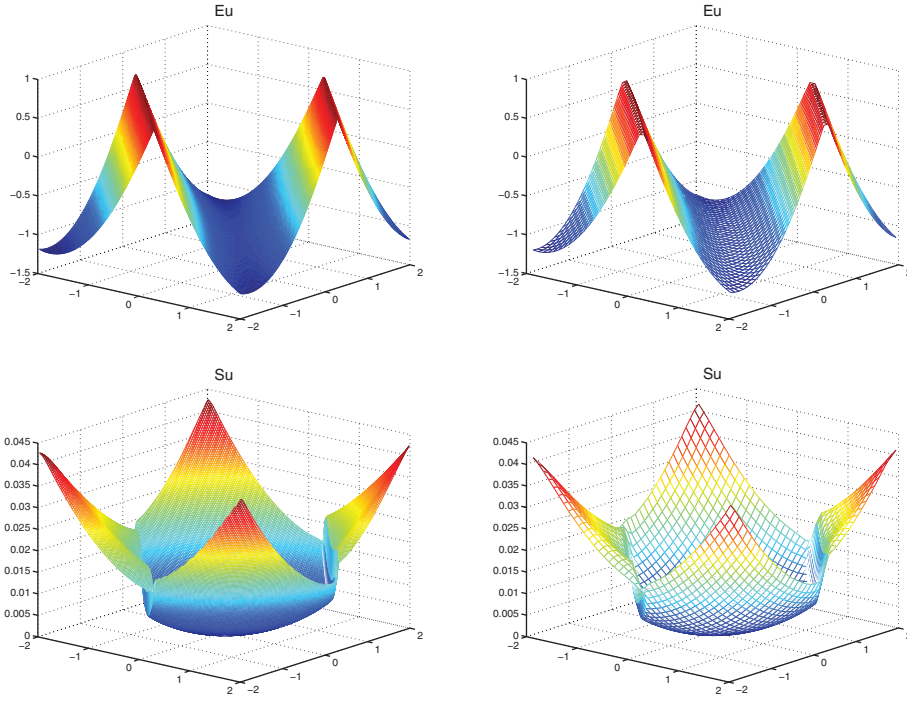


FIG. 11. Example 5. Left: (reference) mean and standard deviation of u by second-order collocation method with $N_x = N_y = 160$, $CFL = 0.4$; right: mean and standard variation of u by second-order Galerkin method with $N_x = N_y = 40$, $CFL = 0.4$.

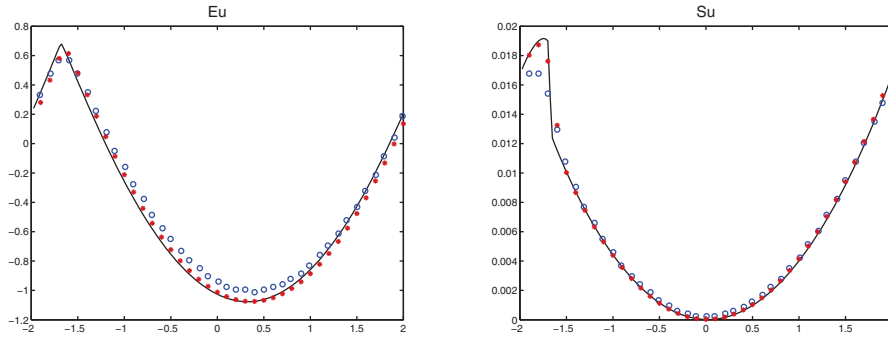


FIG. 12. Example 5. A slice of the solution at $y = 0.5$. Solid line: reference solution; circle: first-order scheme; star: second-order scheme. Left: mean of u ; right: standard deviation of u .

Example 7 (2D Eikonal equation with random wave speed). Consider

$$u_t + H(u_x, u_y, x, y, z) = 0, \quad H(p, q, x, y, z) = c(x, y, z)\sqrt{p^2 + q^2}, \quad (x, y) \in [-2, 2]^2,$$

with random wave speed

$$c(x, y, z) = 1 + \sigma \cos\left(\frac{\pi}{2}xy\right)z, \quad \sigma = 0.2,$$

and deterministic initial data

$$u_0(x, y) = |x| + |y| - 0.5.$$

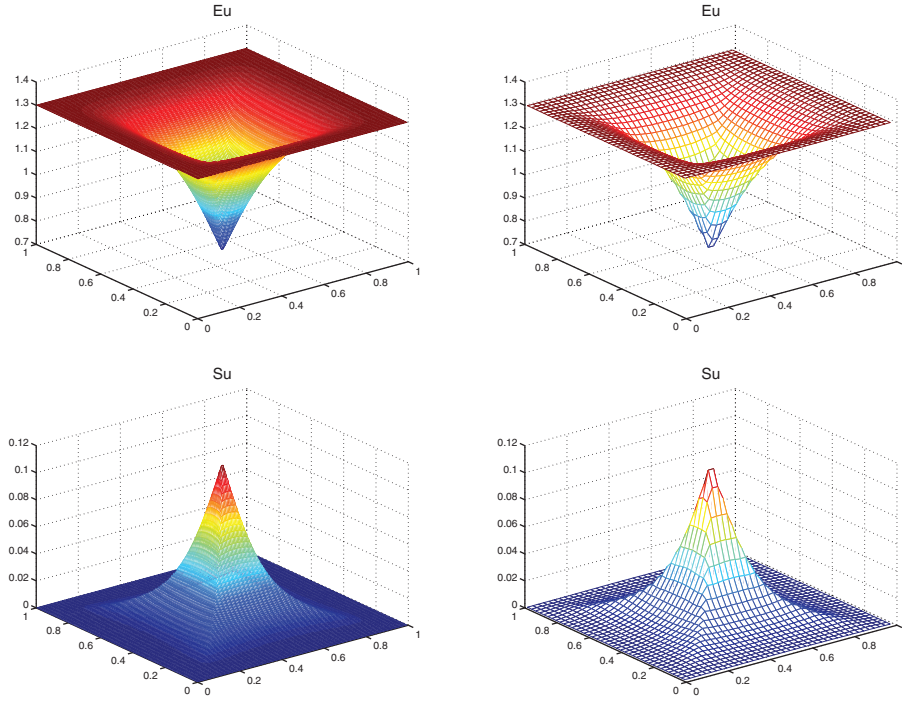


FIG. 13. Example 6. Left: (reference) mean and standard deviation of u by second-order collocation method with $N_x = N_y = 160$, $CFL = 0.4$; right: mean and standard deviation of u by second-order Galerkin method with $N_x = N_y = 40$, $CFL = 0.4$.

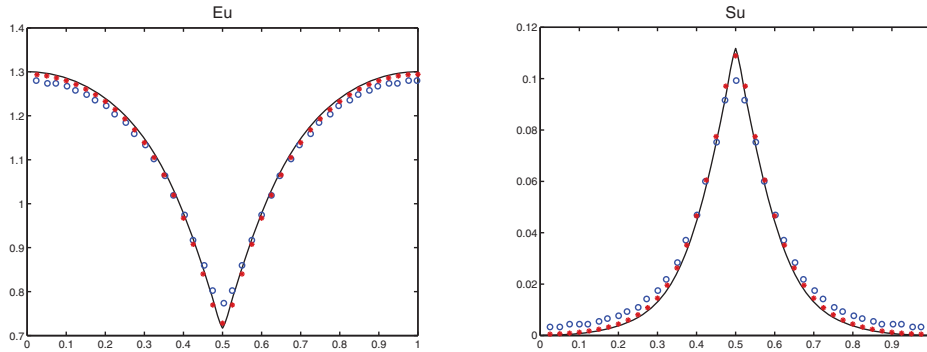


FIG. 14. Example 6. A slice of the solution at $y = 0.5$. Solid line: reference solution; circle: first-order scheme; star: second-order scheme. Left: mean of u ; right: standard deviation of u .

This problem was also modified based on the deterministic example in [28]. We use the second-order scheme with $\alpha = 1.5$, $N = 7$, $N_x = N_y = 80$, $CFL = 0.4$, and compute the solution to $t = 0.9$. For this problem, the initial zero level set of u is a square centered at the origin. The H–J equation describes a solution whose zero level set moves in the outward normal direction with speed $c(x, y, z)$. Since the mean of c is a constant, the mean of u (Figure 15) is more or less the same as the deterministic case. However, if we check the variance, we can get a general idea about the impact of the random input (Figure 16).

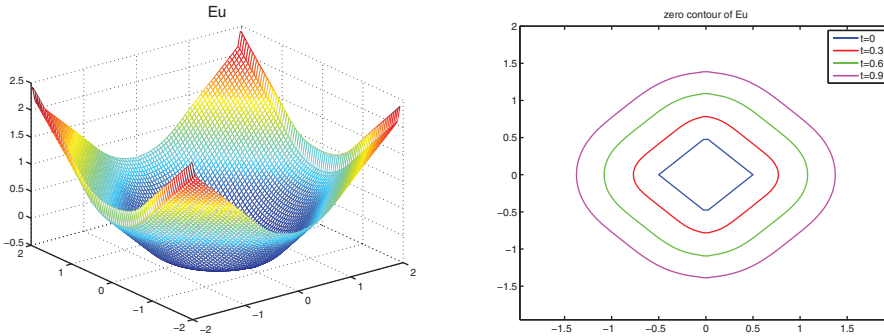


FIG. 15. Example 7. Mean of u by second-order scheme. Left: Three-dimensional (3-D) plot at $t = 0.9$; right: zero level set at $t = 0, 0.3, 0.6, 0.9$.

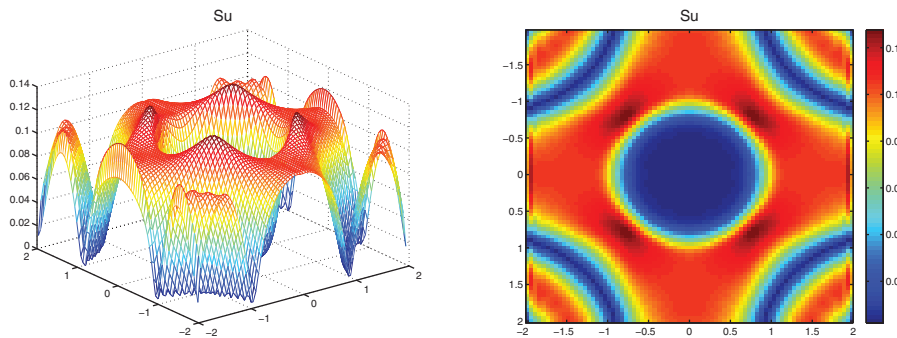


FIG. 16. Example 7. Standard deviation of u at $t = 0.9$ by second-order scheme. Left: 3-D plot; right: bird eye view.

6. Appendix: Proof of Theorem 3.2. To prove the theorem, we first establish the following result.

PROPOSITION 6.1. *The following inequality holds:*

$$(6.1) \quad \begin{aligned} & \frac{1}{2} \partial_t \|p_N(t) - p(t)\|_{L^2(\mathcal{J} \times \mathcal{Z})}^2 \\ & \leq 2 \|H''(p)\|_{L^\infty(\mathcal{J} \times \mathcal{Z})} \|\partial_x p\|_{L^\infty(\mathcal{J} \times \mathcal{Z})} \|p_N - p\|_{L^2(\mathcal{J} \times \mathcal{Z})}^2 \\ & \quad + \|H(p_N)\|_{L^2(\mathcal{J} \times \mathcal{Z})} \|\partial_x(p - \Pi_N p)\|_{L^2(\mathcal{J} \times \mathcal{Z})}. \end{aligned}$$

Proof. The following formula holds in the sense of distribution:

$$(6.2) \quad \begin{aligned} \partial_t \int_{\mathcal{Z}} \frac{1}{2} (p_N - p)^2 d\mu(\mathbf{z}) &= \int_{\mathcal{Z}} \left(\frac{1}{2} \partial_t (p_N)^2 - p_N \partial_t p - p \partial_t p_N + \frac{1}{2} \partial_t p^2 \right) d\mu(\mathbf{z}) \\ &= I_1 + I_2 + I_3 + I_4. \end{aligned}$$

Since p_N is a weak entropy solution, one has

$$I_1 = \int_{\mathcal{Z}} \frac{1}{2} \partial_t (p_N)^2 d\mu(\mathbf{z}) \leq - \int_{\mathcal{Z}} \partial_x \Psi(p_N) d\mu(\mathbf{z}).$$

Since p is a smooth solution, one has

$$I_2 = - \int_{\mathcal{Z}} p_N \partial_t p d\mu(\mathbf{z}) = \int_{\mathcal{Z}} p_N \partial_x H(p) d\mu(\mathbf{z}).$$

In addition,

$$I_3 = - \int_{\mathcal{Z}} p \partial_t p_N d\mu(\mathbf{z}) = - \int_{\mathcal{Z}} \Pi_N p \partial_t p_N d\mu(\mathbf{z}) = \int_{\mathcal{Z}} \Pi_N p \partial_x H(p_N) d\mu(\mathbf{z}),$$

in the sense of distribution, and

$$I_4 = \int_{\mathcal{Z}} \frac{1}{2} \partial_t p^2 d\mu(\mathbf{z}) = - \int_{\mathcal{Z}} \partial_x \Psi(p) d\mu(\mathbf{z}).$$

Therefore, (6.2) gives

$$\begin{aligned} \partial_t \int_{\mathcal{Z}} \frac{1}{2} (p_N - p)^2 d\mu(\mathbf{z}) \\ \leq \int_{\mathcal{Z}} [-\partial_x \Psi(p_N) + p_N \partial_x H(p) + \Pi_N p \partial_x H(p_N) - \partial_x \Psi(p)] d\mu(\mathbf{z}). \end{aligned}$$

Integration in space leads to

$$\partial_t \int_{\mathcal{J} \times \mathcal{Z}} \frac{1}{2} (p_N - p)^2 d\mu(\mathbf{z}) dx \leq \int_{\mathcal{J} \times \mathcal{Z}} [p_N \partial_x H(p) + \Pi_N p \partial_x H(p_N)] d\mu(\mathbf{z}) dx,$$

which can be integrated by parts to give

$$\partial_t \int_{\mathcal{J} \times \mathcal{Z}} \frac{1}{2} (p_N - p)^2 d\mu(\mathbf{z}) dx \leq \int_{\mathcal{J} \times \mathcal{Z}} [p_N \partial_x H(p) - H(p_N) \partial_x \Pi_N p] d\mu(\mathbf{z}) dx.$$

Upon rewriting the right-hand side, we obtain

$$\begin{aligned} \partial_t \int_{\mathcal{J} \times \mathcal{Z}} \frac{1}{2} (p_N - p)^2 d\mu(\mathbf{z}) dx \\ \leq \int_{\mathcal{J} \times \mathcal{Z}} \left[(p_N - p)(H'(p) - H'(p_N)) \partial_x p + \frac{H'(p_N) - \frac{H(p) - H(p_N)}{p - p_N}}{p_N - p} (p_N - p)^2 \partial_x p \right. \\ \left. - H(p) \partial_x p - H(p_N) \partial_x (\Pi_N p - p) + p H'(p) \partial_x p \right] d\mu(\mathbf{z}) dx. \end{aligned}$$

Note, using integration by parts,

$$\begin{aligned} \int_{\mathcal{J} \times \mathcal{Z}} [-H(p) \partial_x p + p H'(p) \partial_x p] d\mu(\mathbf{z}) dx &= 2 \int_{\mathcal{J} \times \mathcal{Z}} p H'(p) \partial_x p d\mu(\mathbf{z}) dx \\ &= 2 \int_{\mathcal{J} \times \mathcal{Z}} \partial_x \Psi(p) d\mu(\mathbf{z}) dx = 0; \end{aligned}$$

we then have

$$\begin{aligned} \partial_t \int_{\mathcal{J} \times \mathcal{Z}} \frac{1}{2} (p_N - p)^2 d\mu(\mathbf{z}) dx \\ \leq \int_{\mathcal{J} \times \mathcal{Z}} \left[(p_N - p)(H'(p) - H'(p_N)) \partial_x p + \frac{H'(p_N) - \frac{H(p) - H(p_N)}{p - p_N}}{p_N - p} (p_N - p)^2 \partial_x p \right. \\ \left. - H(p_N) \partial_x (\Pi_N p - p) \right] d\mu(\mathbf{z}) dx, \end{aligned}$$

which immediately leads to (6.1) (the second term on the right-hand side of (6.1) is obtained by using the Cauchy–Schwarz inequality).

The main result (3.6) is a simple consequence of Proposition 6.1, the assumption (3.5), and the Gronwall inequality. Moreover, (3.7) follows from (3.6) by using the Poincaré inequality.

REFERENCES

- [1] *Engineering Metrology Toolbox*, <http://emtoolbox.nist.gov/Wavelength/Documentation.asp>.
- [2] R. ABGRALL AND P.M. CONGEDO, *A semi-intrusive deterministic approach to uncertainty quantification in non-linear fluid flow problems*, J. Comput. Phys., 235 (2013), pp. 828–845.
- [3] R. ABGRALL, P.M. CONGEDO, AND G. GERACI, *A one-time truncate and encode multiresolution stochastic framework*, J. Comput. Phys., 257 (2014), pp. 19–56.
- [4] K. AKI AND P.G. RICHARDS, *Quantitative Seismology*, 2nd ed., University Science Books, Sausalito, CA, 2002.
- [5] T. BARTH, *Non-intrusive uncertainty propagation with error bounds for conservation laws containing discontinuities*, in Uncertainty Quantification in Computational Fluid Dynamics, Lecture Notes Comput. Sci. Eng. 92, Springer, Heidelberg, 2013, pp. 1–57.
- [6] V. CASELLES, *Scalar conservation laws and Hamilton–Jacobi equations in one-space variable*, Nonlinear Anal., 18 (1992), pp. 461–469.
- [7] Y. CHENG AND C.-W. SHU, *A discontinuous Galerkin finite element method for directly solving the Hamilton–Jacobi equations*, J. Comput. Phys., 223 (2007), pp. 398–415.
- [8] M.G. CRANDALL, L.C. EVANS, AND P.-L. LIONS, *Some properties of viscosity solutions of Hamilton–Jacobi equations*, Trans. Amer. Math. Soc., 282 (1984), pp. 487–502.
- [9] M.G. CRANDALL, H. ISHII, AND P.-L. LIONS, *User’s guide to viscosity solutions of second order partial differential equations*, Bull. Amer. Math. Soc. (N.S.), 27 (1992), pp. 1–67.
- [10] M.G. CRANDALL AND P.-L. LIONS, *Viscosity solutions of Hamilton–Jacobi equations*, Trans. Amer. Math. Soc., 277 (1983), pp. 1–42.
- [11] M.G. CRANDALL AND P.-L. LIONS, *Two approximations of solutions of Hamilton–Jacobi equations*, Math. Comp., 43 (1984), pp. 1–19.
- [12] C.M. DAFLEROS, *Hyperbolic Conservation Laws in Continuum Physics*, Grundlehren Math. Wiss. 235, Springer-Verlag, Berlin, 2000.
- [13] B. DESPRES, G. POETTE, AND D. LUCOR, *Robust uncertainty propagation in systems of conservation laws with the entropy closure method*, in Uncertainty Quantification in Computational Fluid Dynamics, Lecture Notes Comput. Sci. Eng. 92, Springer, Heidelberg, 2013, pp. 105–149.
- [14] L.C. EVANS, *Partial Differential Equations*, 2nd ed., AMS, Philadelphia, 2010.
- [15] R.G. GHANEM AND P. SPANOS, *Stochastic Finite Elements: A Spectral Approach*, Springer-Verlag, New York, 1991.
- [16] D. GOTTLIEB AND D. XIU, *Galerkin method for wave equations with uncertain coefficients*, Comm. Comput. Phys., 3 (2008), pp. 505–551.
- [17] J. JAKEMAN, R. ARCHIBALD, AND D. XIU, *Characterization of discontinuities in high-dimensional stochastic problems on adaptive sparse grids*, J. Comput. Phys., 230 (2011), pp. 3977–3997.
- [18] S. JIN, M.A. KATSOULAKIS, AND Z. XIN, *Relaxation schemes for curvature-dependent front propagation*, Comm. Pure Appl. Math., 52 (1999), pp. 1587–1615.
- [19] S. JIN AND Z. XIN, *Numerical passage from systems of conservation laws to Hamilton–Jacobi equations, and relaxation schemes*, SIAM J. Numer. Anal., 35 (1998), pp. 2385–2404.
- [20] S. JIN, D. XIU, AND X. ZHU, *A stochastic Galerkin method based on relaxation for hyperbolic systems of conservation laws*, preprint, 2014.
- [21] S. JIN, D. XIU, AND X. ZHU, *Asymptotic-preserving methods for hyperbolic and transport equations with random inputs and diffusive scalings*, J. Comput. Phys., 289 (2015), pp. 35–52.
- [22] K.H. KARLSSEN, C. KLINGENBERG, AND N.H. RISEBRO, *A relaxation scheme for conservation laws with a discontinuous coefficient*, Math. Comp., 73 (2004), pp. 1235–1259.
- [23] O. LE MAITRE, O. KNIO, H. NAJM, AND R. GHANEM, *Uncertainty propagation using Wiener–Haar expansions*, J. Comput. Phys., 197 (2004), pp. 28–57.
- [24] O. LE MAITRE, H. NAJM, R. GHANEM, AND O. KNIO, *Multi-resolution analysis of Wiener-type uncertainty propagation schemes*, J. Comput. Phys., 197 (2004), pp. 502–531.

- [25] B. VAN LEER, *Towards the ultimate conservative difference scheme V*, J. Comput. Phys., 32 (1979), pp. 101–136.
- [26] R.J. LEVEQUE, *Finite Volume Methods for Hyperbolic Problems*, Cambridge Texts Appl. Math., Cambridge University Press, Cambridge, 2002.
- [27] O.A. OLENIK, *On the Cauchy problem for weakly hyperbolic equations*, Comm. Pure Appl. Math., 23 (1970), pp. 569–586.
- [28] S. OSHER AND J.A. SETHIAN, *Fronts propagating with curvature-dependent speed: Algorithms based on Hamilton–Jacobi formulations*, J. Comput. Phys., 79 (1988), pp. 12–49.
- [29] S. OSHER AND C.-W. SHU, *High-order essentially nonoscillatory schemes for Hamilton–Jacobi equations*, SIAM J. Numer. Anal., 28 (1991), pp. 907–922.
- [30] B. PERTHAME, N. SEGUIN, AND M. TOURNUS, *A simple derivation of BV bounds for inhomogeneous relaxation systems*, Commun. Math. Sci., 13 (2015), pp. 577–586.
- [31] P. PETTERSSON, G. IACCARINO, AND J. NORDSTRÖM, *A stochastic Galerkin method for the Euler equations with Roe variable transformation*, J. Comput. Phys., 257 (2014), pp. 481–500.
- [32] G. POETTE, B. DESPRES, AND D. LUCOR, *Uncertainty quantification for systems of conservation laws*, J. Comput. Phys., 228 (2009), pp. 2443–2467.
- [33] R. PULCH AND D. XIU, *Generalized polynomial chaos for a class of linear conservation laws*, J. Sci. Comput., 51 (2012), pp. 293–312.
- [34] F. RIZZI, H.N. NAJM, B.J. DEBUSSCHERE, K. SARGSYAN, M. SALLOUM, H. ADALSTEINSSON, AND O.M. KNIO, *Uncertainty quantification in MD simulations. Part I: Forward propagation*, Multiscale Model. Simul., 10 (2012), pp. 1428–1459.
- [35] T. TANG AND T. ZHOU, *Convergence analysis for stochastic collocation methods to scalar hyperbolic equations with a random wave speed*, Commun. Comput. Phys., 8 (2010), pp. 226–248.
- [36] J. TRYOEN, O. LE MAITRE, M. NDJINGA, AND A. ERN, *Roe solver with entropy corrector for uncertain hyperbolic systems*, J. Comput. Appl. Math., 235 (2010), pp. 491–506.
- [37] J. TRYOEN, O. LE MAITRE, M. NDJINGA, AND A. ERN, *Intrusive Galerkin methods with upwinding for uncertain nonlinear hyperbolic systems*, J. Comput. Phys., 229 (2010), pp. 6485–6511.
- [38] X. WAN AND G.E. KARNIADAKIS, *An adaptive multi-element generalized polynomial chaos method for stochastic differential equations*, J. Comput. Phys., 209 (2005), pp. 617–642.
- [39] X. WAN AND G.E. KARNIADAKIS, *Multi-element generalized polynomial chaos for arbitrary probability measures*, SIAM J. Sci. Comput., 28 (2006), pp. 901–928.
- [40] D. XIU, *Numerical Methods for Stochastic Computations*, Princeton Univeristy Press, Princeton, NJ, 2010.
- [41] D. XIU AND G.E. KARNIADAKIS, *The Wiener–Askey polynomial chaos for stochastic differential equations*, SIAM J. Sci. Comput., 24 (2002), pp. 619–644.
- [42] D. XIU AND J. SHEN, *An efficient spectral method for acoustic scattering from rough surfaces*, Commun. Comput. Phys., 2 (2007), pp. 54–72.